

Increasing rate of 21st century volume loss of the Patagonian Icefields measured from proglacial river discharge

Maximillian VAN WYK DE VRIES^{1,2,3}, Matias ROMERO^{4,5,7}, Shanti B. PENPRASE^{1,2}, G.-H. Crystal NG^{1,2}, Andrew D. WICKERT^{1,2,6}

Supplementary Materials

S1: Instrumental evaluation of precipitation data

We correct for any systematic biases in the GPM IMERG remotely sensed precipitation dataset by comparing it with local precipitation gauge data. We select all precipitation gauges from the CRU-TS 4.05 database (Harris et al., 2020) and Argentina's Servicio Meteorológico Nacional within Patagonia south of 45°S, and with an instrumental record covering at least five years of our study period (2000-2020; Figure S1). We identify 11 precipitation gauges meeting these conditions, 6 of which contain monthly data covering the entire study period:

1. Balmaceda - 45.92S 71.70WC
2. Comodoro Rivadavia - 45.78S 67.50W
3. Perito Moreno airport - 46.52S 71.02W
4. Chile Chico - 46.58S 71.69W
5. Puerto Deseado - 47.73S 65.92W
6. Gobernador Gregores airport - 48.78S 70.17W
7. San Julian airport- 49.32S 67.75W
8. Charles Fuhr - 50.27S 71.88W
El Calafate airport - 50.27S 72.05W
9. Rio Gallegos airport - 51.62S 69.28W
10. Punta Arenas - 53.00S 70.85W

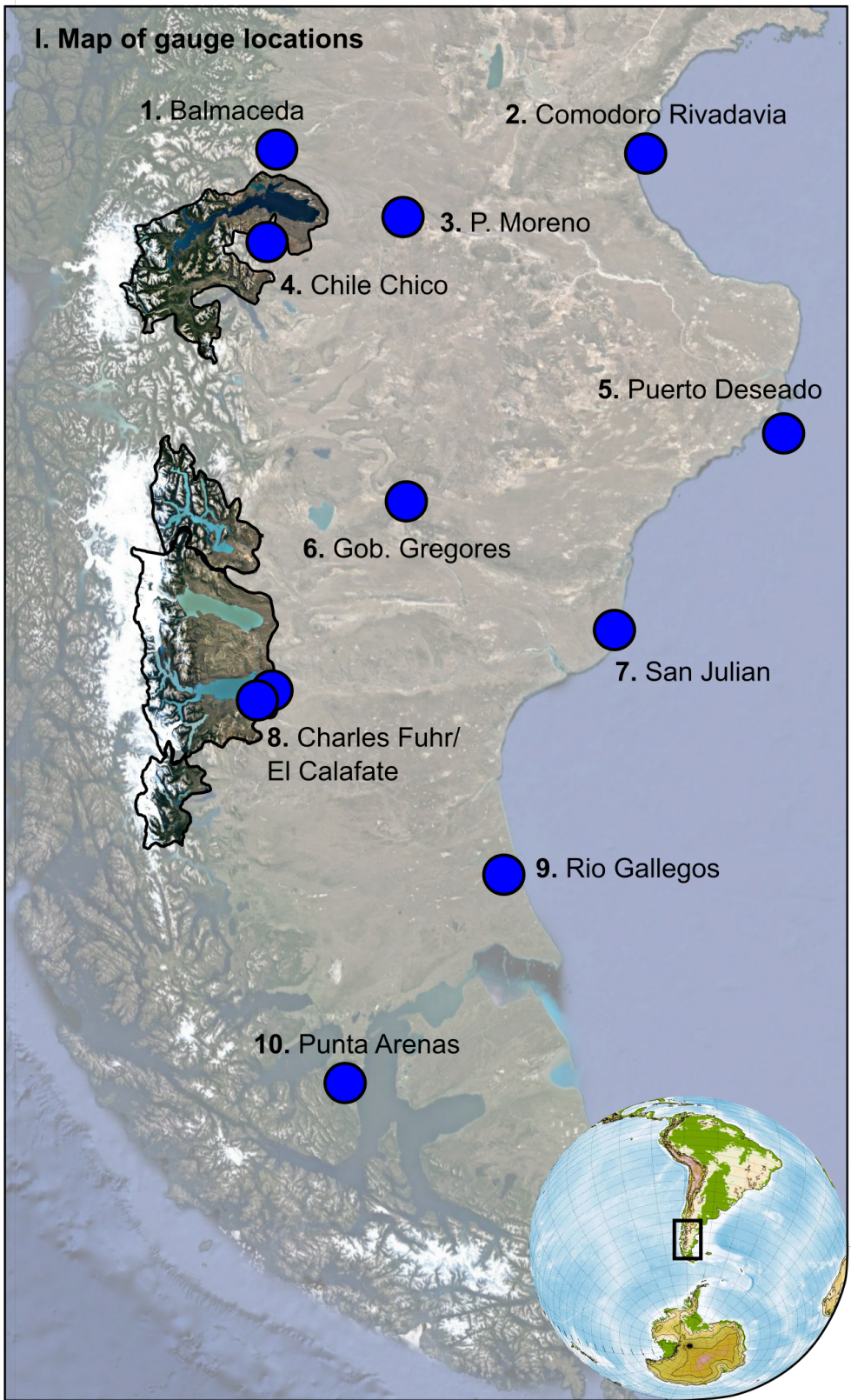


Figure S1: Location of all gages relative to the basins used in this study.

We average the record from two precipitation gages (Charles Fuhr and El Calafate airport) which are located within 10 km of each other. For each precipitation gauge, we download monthly resolution GPM IMERG data from the grid cell nearest to the gauge (Table S1; Figure S2). We use an outlier-robust iteratively reweighted least-squares algorithm to calculate the ratio between instrumental and remotely sensed data. We also calculate the correlation coefficient between these datasets and the final 5-year anomaly (relative to 2000-2005) for each dataset. Two gauges (2 and 8) only cover the period prior to 2010, and so we do not calculate an anomaly. Too few gauges are available to calculate an individual correction factor for each sub-basin, and so we use the overall correction factor of GPM IMERG precipitation = 2.25 gauge precipitation, or a correction of 0.44.

Table S1: Comparison between GPM and precipitation gauge data.

Gauge number	Average GPM to gauge ratio	Correlation coefficient (GPM,gauge)	last 5 yr anomaly GPM	last 5 yr anomaly gauge
1	1.36	0.86	0.77	0.86
2	2.74	0.76	1.02	0.89
3	1.84	0.81	0.75	0.60
4	2.31	0.74	0.70	
5	2.99	0.78	0.80	1.08
6	1.50	0.83	1.06	
7	1.90	0.82	0.76	0.80
8	1.91	0.57	0.46	0.89
9	2.21	0.83	1.01	0.93
10	2.58	0.70	0.80	0.69
All	2.28	0.81	0.81	0.84

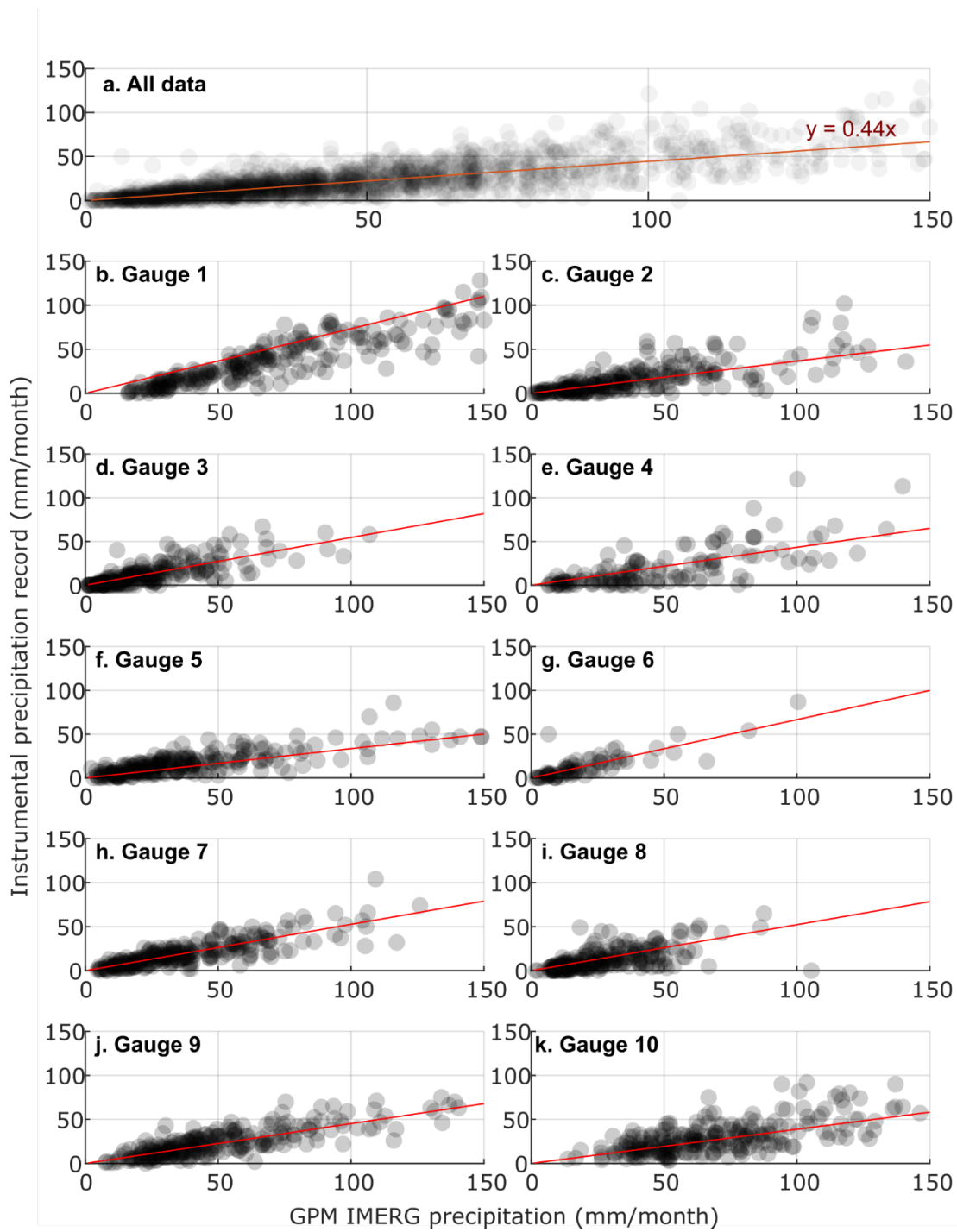


Figure S2: Plot of gauge precipitation data against GPM precipitation data for each of the 10 gauges and all data from the region.

S2: Evaluation of temperature change in Southern Patagonia

We obtained temperature and precipitation covering the period 1940-2020 from the CRU-TS 4.05 monthly time series with a spatial resolution of half a degree (~50 km). This dataset combines records from several meteorological stations around Southern Patagonia into a single homogeneous record. For each sub-basin we selected the half-degree grid cell covering the largest fraction of its glacier area.

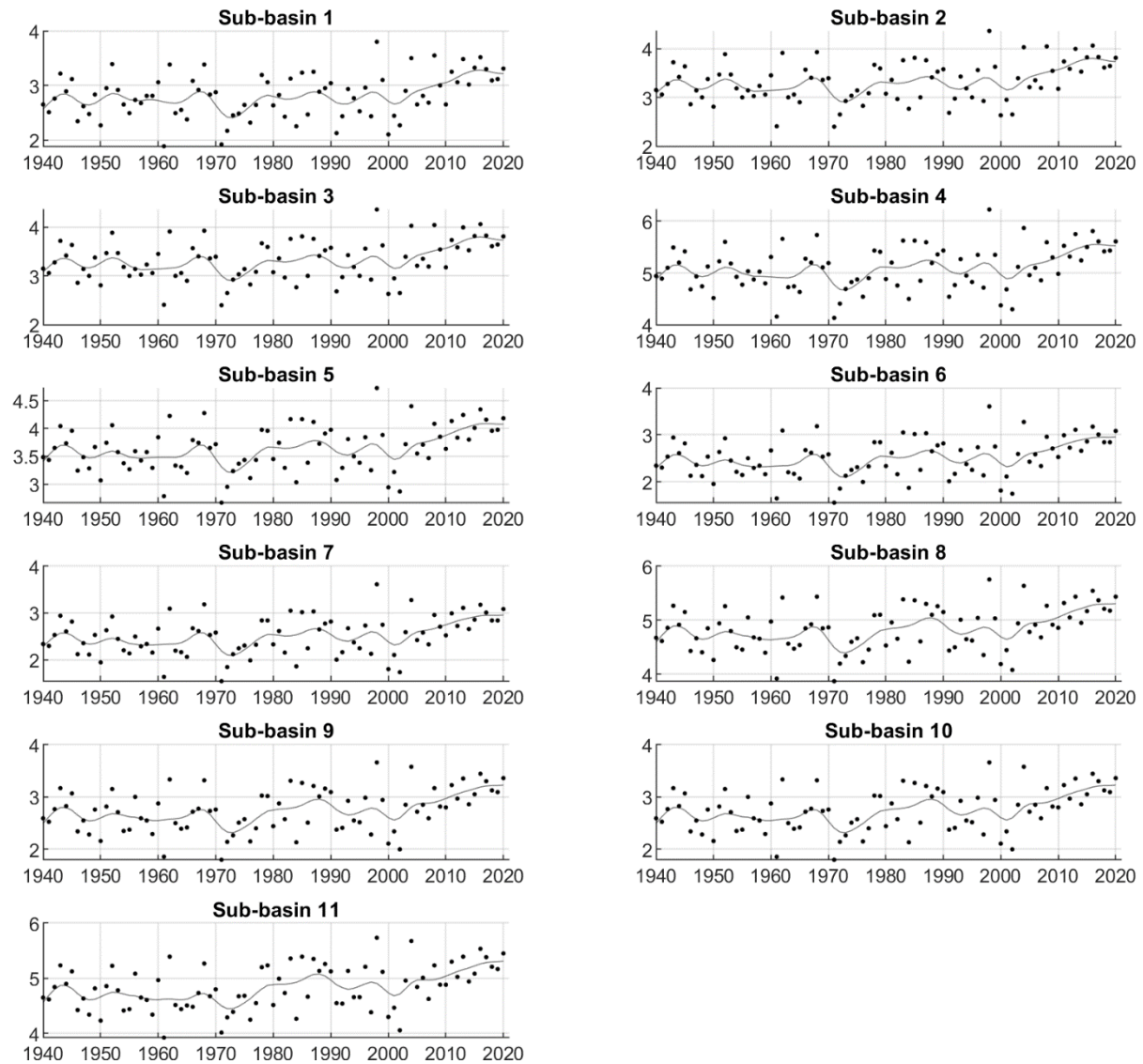


Figure S3: Temperature change in degrees C from 1940 to 2020 for each sub-basin in our study area. Points represent mean annual temperatures, while the grey line represents a 10-year gaussian smoothed temperature timeseries. A sustained period of warm years from 2005-2020 is visible in all sub-basins.

Table S2: Temperature anomalies at the 11 sub-basins relative to two different reference periods.

Sub-basin number	2006_2010 relative to 1940_1980	2010_2015 relative to 1940_1980	2015_2019 relative to 1940_1980	2006_2010 relative to 2000_2005	2010_2015 relative to 2000_2005	2015_2019 relative to 2000_2005
1	0.36	0.48	0.53	0.33	0.45	0.50
2	0.38	0.49	0.57	0.35	0.46	0.54
3	0.38	0.49	0.57	0.35	0.46	0.54
4	0.26	0.47	0.58	0.27	0.47	0.58
5	0.28	0.48	0.58	0.25	0.45	0.56
6	0.27	0.47	0.57	0.24	0.44	0.54
7	0.27	0.47	0.57	0.24	0.44	0.54
8	0.25	0.48	0.62	0.18	0.41	0.54
9	0.25	0.49	0.63	0.16	0.40	0.54
10	0.25	0.49	0.63	0.16	0.40	0.54
11	0.23	0.48	0.64	0.11	0.36	0.52

S3: Ice volume in individual sub-basins

We calculate ice thickness within each sub-basin by clipping Millan et al., 2019's 'full thickness' grid to the extent of each sub-basin. This full thickness grid is based on Millan et al., 2019's gravity inversion where data is available, combined with Carrivick et al., 2016's flowline model based thickness calculation for areas of missing data.

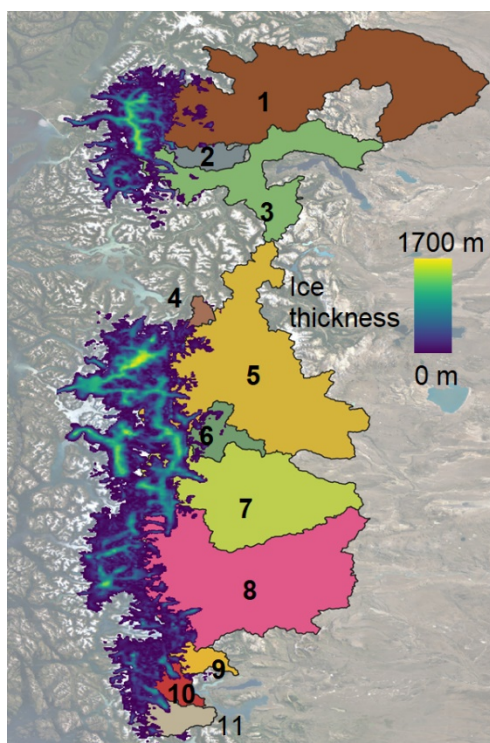


Figure S4: Ice thickness of the Patagonian icefields relative to the location of our 11 sub-basins. Data from Millan et al., 2019.

Table S3: Ice area and volume in each sub-basin.

Sub-basin	Total area (km ²)	Glacierized area (km ²)	Fraction ice cover	Volume (km ³)
1	8776	714	8	46
2	892	177	20	49
3	4270	683	16	140
4	390	119	31	16
5	8307	2471	30	753
6	1048	307	29	8
7	6362	1077	17	564
8	9678	1875	19	565
9	757	160	21	23
10	826	439	53	135
11	1148	440	38	124

S4: List of abbreviations and symbols

SPI = Southern Patagonian Icefield

NPI = Northern Patagonian Icefield

rGVL = relative glacier volume loss

GPM IMERG = Global Precipitation Mission Integrated Multi-satellitE Retrievals

MODIS = Moderate Resolution Imaging Spectroradiometer (Terra)

MOD16A2 = MODIS derived evapotranspiration dataset

GRACE = Gravity Recovery and Climate Experiment